

zones depends on the particular choice of source latitude, source spectrum, and source solid angle.

There is the additional comment that at 50 degrees latitude, the 0900 impact zone receives higher rigidity particles, the 0300 impact zone lower rigidity particles, whereas at latitude 60 degrees, both the high and the low rigidity particles are received in the 0900 zone. This tendency for observers at middle latitudes to see monoridity solar flare particles, and observers at higher latitudes (60 degrees) to see the integrated spectrum, is not too sensitive to source latitude and source solid angle.

ACKNOWLEDGMENTS

The writer wishes to express his thanks to Professor J. A. Simpson for continued support and many encouraging discussions. The orbit program would not have been possible without the stimulating and generous help of Dr. D. Flanders of Argonne National Laboratory. For programming of the orbit integration we are very grateful to Mrs. R. Freshour of the AVIDAC staff. We are deeply indebted to M. Pyka, M. Baker, and J. Ayres of this laboratory for aid in obtaining and preparing the results.

PHYSICAL REVIEW

VOLUME 103, NUMBER 4

AUGUST 15, 1956

Heavy Primary Cosmic Radiation at the Equator*

R. E. DANIELSON,[†] P. S. FREIER, J. E. NAUGLE, AND E. P. NEY

Department of Physics, University of Minnesota, Minneapolis, Minnesota

(Received April 16, 1956)

The zenith and azimuthal angular distribution of primary cosmic rays with charges ≥ 6 has been measured at the equator using oriented nuclear emulsions. The magnitude of the azimuthal asymmetry is consistent with an integral power law spectrum which falls off inversely as the 2.0 power of the total energy per nucleon. However, the maximum intensity comes from the southwest rather than the west. This is consistent with the recently proposed shift of the earth's effective magnetic field for cosmic rays.

The flux at the top of the atmosphere is 0.68 particle $\text{m}^{-2} \text{sec}^{-1} \text{sterad}^{-1}$ for CNOF (carbon, nitrogen, oxygen, fluorine) nuclei and 0.21 particle $\text{m}^{-2} \text{sec}^{-1} \text{sterad}^{-1}$ for nuclei with $Z \geq 10$.

INTRODUCTION

EARLY counter measurements¹ of east-west asymmetries have always resulted in asymmetries which are smaller than that predicted by geomagnetic theory, assuming that the incident flux is isotropic and that all the primary cosmic rays are positively charged. Part of this discrepancy is no doubt caused by non-primary radiation² in the form of secondary particles, resulting from interactions with air nuclei, which enter the counter telescope from below. This effect would be especially large at large zenith angles, and this is where the discrepancy is the greatest. If one were to measure the asymmetries of heavy nuclei, however, one could be certain as to the primary character of the particles. Therefore an orienter was designed to orient horizontal nuclear emulsions with respect to the earth's magnetic field.

A second purpose of this experiment was to measure the primary flux of the heavy component at the equator. This flux measurement constitutes an important point on the integral energy spectrum for the heavies.

A knowledge of the analytic form of this integral energy spectrum is important since the exponent in the proper law (if one assumes that a power law of the total energy is the correct analytical form) appears to be larger for heavy primaries than for protons. This would be useful information concerning the acceleration mechanism and lifetime of the primary cosmic radiation.

The third purpose of this experiment was to resolve the charge spectrum as much as possible. This is of interest since the comparison of relative abundances of the elements in the primary cosmic radiation at various energies with the observed abundances in the universe is valuable information concerning the lifetime and sources of cosmic radiation. Any marked deviation of the abundances of the components of the cosmic rays from the observed abundances in the universe provides important data in devising an origin theory.

BALLOON FLIGHTS AND APPARATUS

Two balloon flights were flown as part of Project Churchy, a cosmic-ray expedition to the Galapagos Islands near the geographic equator. The time-altitude curve for Flight 2 is shown in Fig. 1. The flight record for Flight 1 is similar. The trajectory of the balloon was approximately straight from the launch point (geographic latitude $0^{\circ}20'S$; geographic longitude $90^{\circ}20'W$) to the splash point ($1^{\circ}20'S$; $96^{\circ}10'W$).

* This work supported in part by the joint program of the U. S. Atomic Energy Commission and the Office of Naval Research.

[†] National Science Foundation predoctoral fellow, 1955-1956. This work was carried out in partial fulfillment of the requirements for the Master's degree.

¹ Winckler, Stix, Dwight, and Sabin, *Phys. Rev.* **79**, 666 (1950).

² K. A. Anderson, Ph.D. thesis, University of Minnesota, 1955 (unpublished).

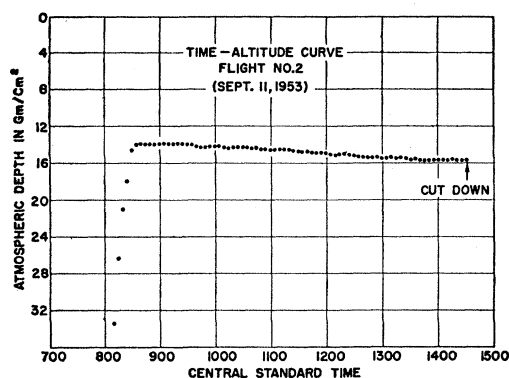


FIG. 1. Time-altitude curve for flight of September 11, 1953. The probable error of each point in 0.3 g/cm^2 .

The orientation-sensing mechanism consisted of a compass and two photocells arranged so that when the apparatus drifted away from the oriented direction, one of the photocells was illuminated. This signal was amplified and used to switch the orienting motor on and off by means of a differential relay. The recorder mechanism photographed a pressure gauge, a watch, a level, a thermometer and a compass. The compasses were placed in the gondola in such a manner that they did not interact. The entire equipment was contained in a 30-inch pressurized and insulated aluminum sphere. The entire sphere was oriented against two weights suspended on the ends of a six-foot boom. The emulsions consisted of six 4×10 -inch stacks of three 600-micron emulsions arranged horizontally on the equatorial plane of the 30-inch aluminum sphere and were flown horizontally in order to facilitate measurements of the azimuthal asymmetry. For purpose of charge identification, vertical plates would have been better since one observes a larger number of long tracks in vertical plates than in horizontal plates.

CHARGE SPECTRUM

Since the cutoff at the equator is about 6 Bev/nucleon, all of the primary particles are relativistic, and therefore the delta-ray density will vary as Z^2 . Over four-hundred primaries were delta-ray-counted over their entire length in the stack. The results of these counts are shown in Fig. 2. It appears that the CNOF region (carbon, nitrogen, oxygen, and fluorine) is on the verge of being resolved, but if it is resolved, the case is

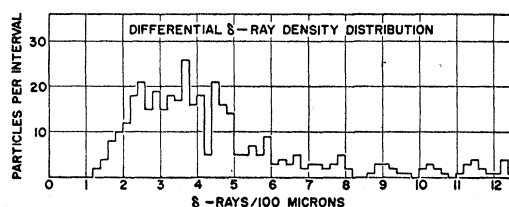


FIG. 2. Differential δ -ray density distribution for particles at $\lambda = 10^\circ \text{N}$.

not very convincing. However, even though neighboring charges aren't resolved, the general features of the charge spectrum are significant; and the δ -ray densities serve to classify the nuclei as to whether they are in the CNOF group or in the $Z \geq 10$ group. Resolution of charge was obtained, however, when the particles with zenith angles greater than 68° (total path length in stack greater than 4 mm) were analyzed in the manner described below.

If one assumes that the entire error in delta-ray counting results from random fluctuations in the number of delta rays counted, one would want to plot a Gaussian curve for each particle and add up the Gaussians corresponding to the individual particles. In order to adapt this problem to the digital computer available, the Gaussian distribution for a single particle was approximated by a parabola. The equation for a normalized Gaussian error curve is given by

$$y_g = \frac{1}{(2\pi)^{1/2}\sigma} \exp\left[-(x-x_0)^2/2\sigma^2\right], \quad (1)$$

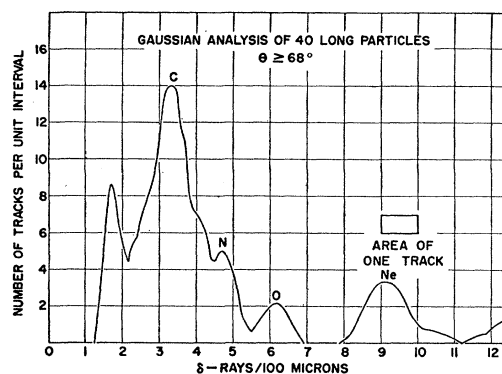


FIG. 3. Gaussian analysis of 40 long tracks with $\theta \geq 68^\circ$.

where x_0 is the observed delta-ray density and σ is the standard deviation. A normalized parabolic approximation given by

$$y_p = \frac{3}{8\sigma} [1 - (x-x_0)^2/4\sigma^2] \quad (2)$$

is a reasonably good approximation to the Gaussian error curve and has no sharp corners such as a triangle would have. The above analysis was performed on 40 long tracks using the parabolic approximation. The result is shown in Fig. 3. The four peaks are identified as carbon, nitrogen, oxygen, and neon. The little peak occurring at a delta-ray density of about 1.7 is not significant since the scanning cutoff was set at 2.5 delta rays per 100 microns. The above identifications are consistent with an interaction observed in the emulsion in which a heavy particle collides with an emulsion nucleus and forms a lighter fragment plus two protons and one alpha particle. The incoming particle has a

delta-ray density corresponding to neon, while the outgoing fragment has a delta-ray density corresponding to carbon.

The 400 particles were also divided up into three groups according to zenith angle. The Z spectrum was resolved for all the particles with zenith angles greater than 60 degrees with the same result as for the very long particles in the entire stack. By noting where the carbon peak appeared to be in the other zenith angle intervals ($5 \leq \theta \leq 40$ and $40 \leq \theta \leq 60$), the average calibration for the 400 particles was found to be

$$N = 0.10Z^2, \quad (3)$$

where N is the number of delta rays per 100 microns. Using this calibration, one can see from Fig. 2 that the ratio of the CNO components is roughly

$$C:N:O::3:2:1.$$

This is to be compared with the abundance ratios of the CNO group as determined from the earth's crust, from meteorites and from stellar atmospheres. This ratio is³

$$C:N:O::1:2:6.$$

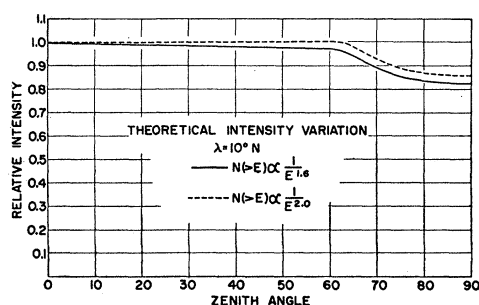


FIG. 4. Average azimuthal intensity as a function of zenith angle.

Thus the abundance ratio of the high-energy component of the heavies appears to be just opposite that of the bulk of matter in the universe. To change a ratio of 1:2:6 to 3:2:1 by collisions would take several collision mean free paths at least. It is difficult to calculate how much matter would be needed since one would have to know the probabilities for each $Z \geq 10$ going to C, N, and O separately and for oxygen going to C and N as well.

MEAN FREE PATH

For a given zenith angle, geomagnetic theory predicts that the cutoff will vary with the azimuth angle and will be smallest in the west and largest in the east. If one averages the cutoff (and thus the intensity) around the entire 360 degrees, one will find that the average intensity remains very nearly constant with zenith angle. Figure 4 shows the results of such an averaging for a geomagnetic latitude of $10^\circ N$. One can see that

³ L. H. Aller, *Astrophysics* (Ronald Press Company, New York, 1953), Vol. I.

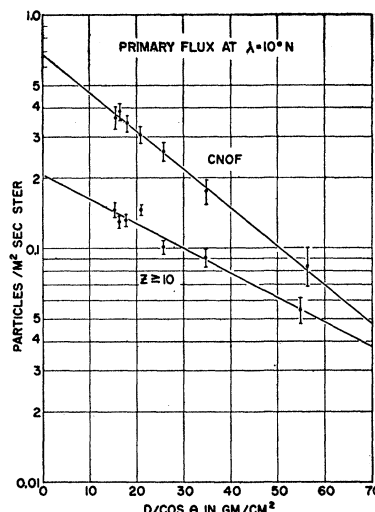


FIG. 5. Zenith angle distribution for CNOF and $Z \geq 10$ at $\lambda = 10^\circ N$.

the average intensity is essentially constant down to a zenith angle of 60 degrees and is less than 20% off at a zenith angle of 80 degrees, below which very few particles enter because of atmospheric absorption. Therefore, one can measure the mean free path of the heavies since the observed intensity should decrease very nearly as $e^{-D/\lambda \cos \theta}$, where λ is the interaction mean free path, D is the average atmospheric depth of the balloon at altitude, and θ is the zenith angle. (The length for stopping by ionization is much too long to be important at the particle energies which are allowed at a geomagnetic latitude of $10^\circ N$.) Thus a plot of the log of the observed intensity versus $D/\lambda \cos \theta$ should be a straight line if the incident flux is isotropic and should intersect at $D/\lambda \cos \theta = 0$ to give the cosmic-ray intensity at the top of the atmosphere.

Figure 5 shows the results for the CNOF and $Z \geq 10$ components for Flight 2. (Flight 2 was the better oriented of the two flights.) The least squares analysis produced the results in Table I.

The value of about 40 g/cm² for the mean free path in air of the $Z \geq 10$ component is about twice that previously measured by the same method at Cuba ($30^\circ N$) and at Minnesota ($55^\circ N$) by Freier *et al.*⁴ The values that they obtained were 19 g/cm² at $55^\circ N$ (Minnesota) and 21 g/cm² at $30^\circ N$ (Cuba). Noon and Kaplon⁵ have recently measured the interaction mean free paths for heavy particles in emulsion at Texas

TABLE I. Flux and mean free path at the equator.

Charge	Flux at top of atmosphere (particles/m ² sec sterad)	Mean free path in air (g/cm ²)
CNOF	0.68 ± 0.06	26 ± 2
$Z \geq 10$	0.21 ± 0.05	41 ± 5

⁴ Freier, Anderson, Naugle, and Ney, *Phys. Rev.* **84**, 322 (1951).

⁵ J. H. Noon and M. F. Kaplon, *Phys. Rev.* **97**, 769 (1955).

TABLE II. Emulsion mean free path at equator.

Charge	Total path length (cm)	Number of interactions	λ g/cm ²	λ_{theor} g/cm ²
CNOF	99.9	7	57	48
$Z \geq 10$	66.1	3	88	36

(41°N) and at Minnesota (55°N). Their results are energy insensitive up to 6 Bev/nucleon and are consistent with the following expression for the interaction cross section:

$$\begin{aligned}\sigma &= \pi[R_i + R_t - 2\Delta R]^2 \text{ cm}^2, \\ \Delta R &= 0.85 \times 10^{-13} \text{ cm}, \\ R &= 1.45 \times 10^{-13} A^{\frac{1}{3}} \text{ cm}.\end{aligned}\quad (4)$$

If one uses Noon and Kaplon's relation, one computes the following interaction mean free paths in air assuming an average Z of 7 for the CNOF group and an average Z of 15 for the $Z \geq 10$ group.

$$\begin{array}{ll}\text{CNOF} & 27 \text{ g/cm}^2, \\ Z \geq 10 & 19 \text{ g/cm}^2.\end{array}$$

Thus the calculated mean free path for the CNOF component agrees with the measured value while the measured value for the $Z \geq 10$ component is larger by a factor of two than the calculated value.

The anomalously long mean free path obtained for heavies at the equator may have several explanations:

(1) The mean free path measured from the zenith angular distribution is an absorption mean free path. When a nucleus in the CNOF group interacts, it has a high probability of being removed from the group, while a nucleus in the $Z \geq 10$ group can reduce its charge in a collision and may still stay in the $Z \geq 10$ group. This explanation would seem logical if we had not measured the absorption mean free path in Cuba as 21 g/cm². The average energy is lower at Cuba, but in order for the mean free paths to be so different at the two places, the cross section would have to suddenly become energy dependent (and smaller) at an energy

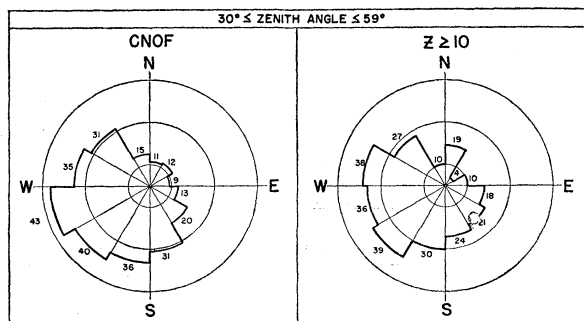


FIG. 6. Azimuthal asymmetries measured at the equator for primaries with zenith angles between 30° and 60° on flight of September 11, 1953.

of about 6 Bev/nucleon; or the charge spectrums would have to be different at the two places.

(2) The long mean free path may be due to the fact that the mean free path at the equator was measured with horizontal plates, while the other (and shorter) mean free paths were measured on vertical plates. However, in one flight at Minnesota on April 13, 1950, (at a residual depth of 14 g/cm²) the angular distribution was measured on both horizontal and vertical plates for the purpose of checking the relative efficiencies of the two detectors. The results based on 1236 and 803 nuclei, respectively, gave the same flux and mean free path. The only discrepancy occurred at zenith angles less than 20°, where the horizontal plate gave a low result as one would expect.

(3) The long mean free path for the $Z \geq 10$ component may be due to an anisotropy in the high-energy primary nuclei. The method used in the measurement of the mean free path involved the assumption that the primary flux was isotropic and that geomagnetic theory

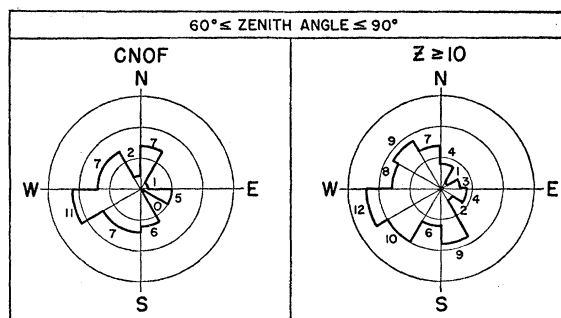


FIG. 7. Azimuthal asymmetries measured at the equator for primaries with zenith angles $\geq 60^\circ$ on flight of September 11, 1953.

was valid. If either of these assumptions were not valid, then one could question the observed result. Any deviation from geomagnetic theory, however, should affect both the $Z \geq 10$ components and CNOF components in the same way since they are both composed of nuclei with $A = 2Z$. Thus the geomagnetic effects seem to be eliminated. The observed asymmetries (to be discussed in the next section) of the CNOF and $Z \geq 10$ group appear to be the same, however, so if anisotropy is the true reason for the long mean free path, it is indeed fortuitous that the experiment happened to be performed at just the time of day and year so that the asymmetries appeared to look the same and yet yielded different mean free paths.

In an attempt to determine whether the long $Z \geq 10$ mean free path was really correct, we measured the mean free path in emulsion even though the statistics were very poor. It is to be noted that we followed many particles a short distance (horizontal plates) in order to get these results given in Table II. In the emulsion, also, the mean free path for the $Z \geq 10$ appears signifi-

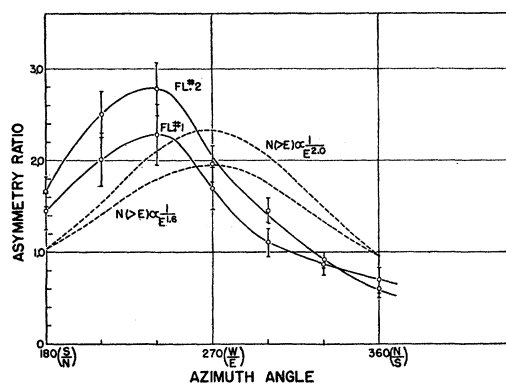


FIG. 8. Azimuthal asymmetries obtained for $Z \geq 6$ by comparing intensities in opposite hemispheres for zenith angles between 30° and 60° .

cantly larger than the calculated value, while the CNOF value appears to agree with the calculated value.

The scanning criteria was set so as to detect all nuclei with charge greater than or equal to 6. The zenith angle distribution shows that some CNOF nuclei were missed in the interval from $0-20^\circ$. A check of the scanning efficiency showed that about 10% of the CNOF group were missed and that all the missed ones had zenith angles less than 30° .

Figure 2 shows that many particles with ionization less than that of carbon were also found in the scan. Most of these were followed and δ -ray counted over ranges long enough to rule out their being slow evapora-

tion alpha particles. These particles were analyzed by the same method used for the other charge groups. The flux at the top of the atmosphere was 0.4 ± 0.1 particles/m² sec sterad, while the corresponding mean free path was between 25–30 g/cm² of air. Thus, in spite of the fact that the scanning was inefficient for Be and B nuclei, an appreciable flux of these particles was observed.

ASYMMETRIES

Neither of the two flights was perfectly oriented. A detailed analysis showed that the second flight was the better oriented of the two. Although it is not rigorously correct to do so, each flight was analyzed into the percentage time-oriented and the percentage time-random. The percentages of time-oriented were 38% for Flight 1 and 73% for Flight 2.

Figure 6 shows the azimuthal entrance angle distribution for zenith angles from 30 to 59 degrees for Flight 2. In this graph the 27% randomness has been subtracted out. Figure 7 shows the same result for zenith angles greater than 60° . One can see that the distributions show an asymmetry, with the maximum number coming from the southwest rather than from the west as expected. To try to verify this unexpected asymmetry, Flight 1 was analyzed in the same manner as the other flight except that the particles were classified into charge groups by inspection rather than by delta-ray counting. In spite of the fact that 62% of the particles were subtracted away, this flight also shows the maximum from the same direction.

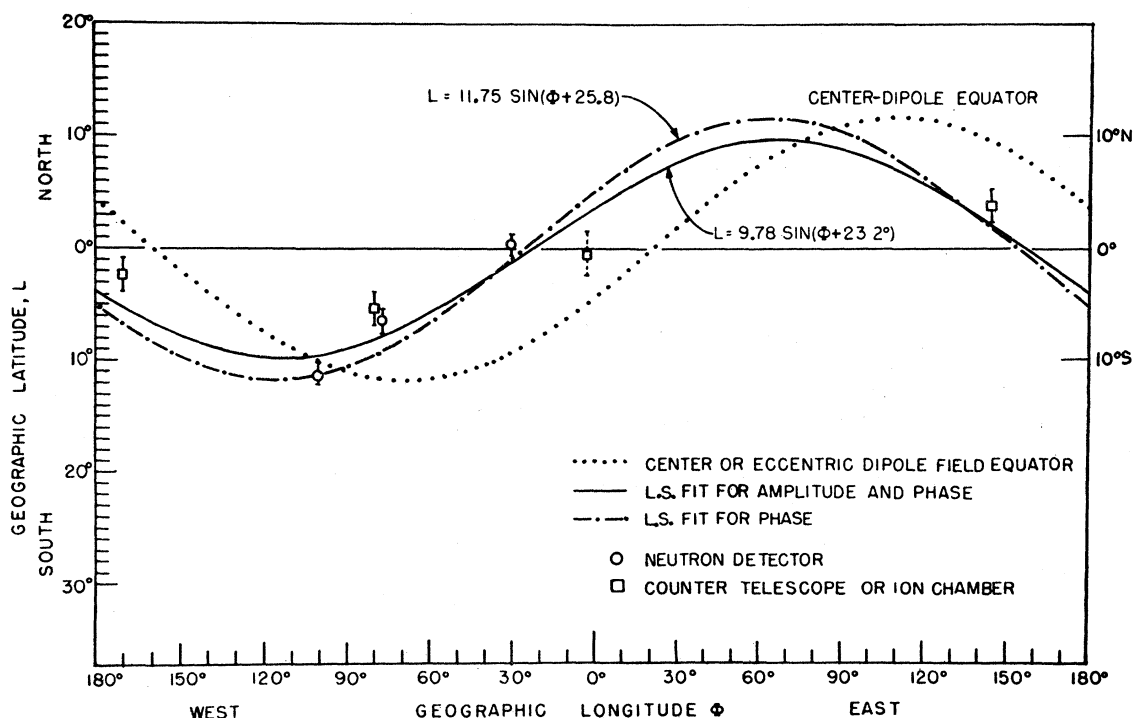


FIG. 9. Schematic sketch of the loci of the equators for the equivalent dipole field and the proposed cosmic-ray dipole field.

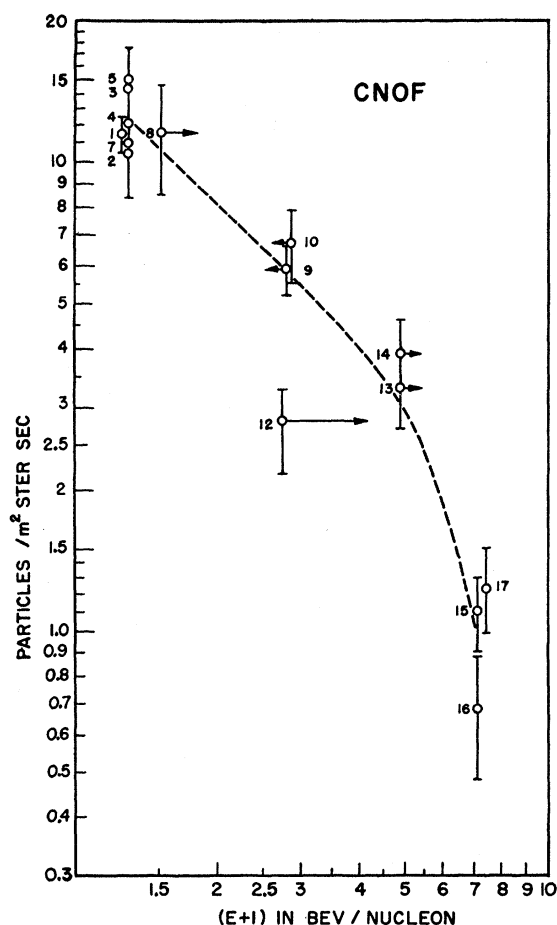


FIG. 10. Energy spectrum for the CNOF group.

Another comparison of the two flights may be obtained by computing the ratios of the flux entering in opposite hemispheres as a function of azimuth angle. This is shown in Fig. 8, along with the ratios expected when one assumes power law spectra which fall off inversely as the 1.6 and 2.0 power of the total energy per nucleon and assuming isotropy of the primaries at infinity.

By comparing the observed ratios with the predicted ratios, one can see that the observed asymmetry ratio is slightly larger than one would expect from geomagnetic theory for an integral energy spectrum with an exponent of 1.6 and would be more in agreement with an exponent of about 2.0.

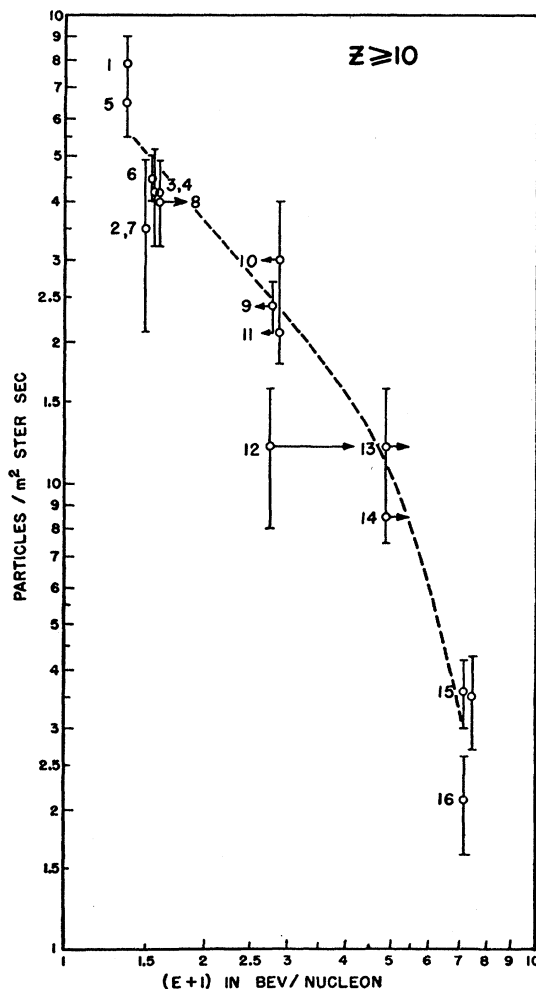
The direction of the asymmetry corroborates some recent work of Simpson and Rose,^{6,7} indicating that the geomagnetic equator as determined by the minimum sea level neutron count does not coincide with the previously accepted geomagnetic equator. Their data indicate that the cosmic-ray dipole is tipped with

⁶ Simpson, Jory, and Pyka, *J. Geophys. Research* (to be published).

⁷ Simpson, Fenton, Katzman, and Rose, *Phys. Rev.* **102**, 1638 (1956).

respect to the surface dipole field in such a way that the geomagnetic latitude of England (0° longitude) is about 6° lower than had been previously assumed.⁸

Figure 9 shows schematically the old geomagnetic equator along with Simpson's proposed cosmic-ray equator.⁹ Since this experiment was performed at a longitude of 90° W, one can see that the geomagnetic latitude remains the same. The plates were oriented with respect to the surface field (which at this point coincides with the equivalent dipole field to within 4°), while the cosmic rays would be deflected by the "cosmic-ray dipole field." Thus one can see that the asymmetry would be shifted such that the maximum number of particles entered from the southwest rather than from the west. However, our measured shift appears to be larger than the approximately 15° shift which the proposed dipole tip would require.

FIG. 11. Energy spectrum for the $Z \geq 10$ group.

⁸ C. J. Waddington, *Nuovo cimento* **3**, 930 (1956).

⁹ We wish to thank Dr. Simpson⁷ for the use of this figure prior to his publication of it.

FLUX AND ENERGY SPECTRUM

If the heavy component is not isotropic, then the flux values obtained by extrapolating to the top of the atmosphere using the mean free paths derived from the zenith angular distribution will not be correct. In this case one would have to specify the direction in quoting a flux. If one supposes, however, that the magnetic field which influences the cosmic rays is effectively a dipole field (which does not coincide with the previously accepted dipole field), then the fluxes obtained by extrapolating to the top of the atmosphere with the derived mean free path are valid. The fluxes obtained in this way are given in Table I.

These flux values as well as others previously obtained have been plotted in Figs. 10 and 11 to form an integral energy spectrum.

Table III gives the flux values plotted on the graph. We have included all the flux values we found in the literature, but we do not guarantee the completeness of the list. λ is the geomagnetic latitude, and the new value of λ is based on Simpson's proposed cosmic-ray dipole. E_c is the cutoff energy in Bev/nucleon. The "a" after the value means that the cutoff energy is imposed by the air above the detector rather than by the earth's magnetic field. The fluxes are divided into the CNOF group and the $Z \geq 10$ group, since we find a low abundance of fluorine and have used this as a natural place to divide the nuclei into two groups. If the quoted flux value included $Z=10$ with the CNOF group, we have corrected the quoted value using the average abundance of $Z=10$ we measured on two flights, one at $\lambda=55^\circ\text{N}$ and one at $\lambda=15^\circ\text{N}$. (This correction means multiplying the quoted $6 \leq Z \leq 10$ flux by 0.95 to convert it to CNOF; and multiplying $Z > 10$ flux by 1.16 to convert it to $Z \geq 10$ flux.)

It can be seen that for neither of the charge groups does a power law appear to represent the data well, although the data might be consistent with an exponent of 1.6. It is interesting to note that the curve drawn through the data appears to vary as $1/E$ at low energies (which is similar to the proton spectrum) while at high energies the data vary more like $1/E^2$ or even steeper. This is consistent with the data in Fig. 8, which suggests

TABLE III. Flux values for heavy primaries.* Numbers under reference refer to corresponding numbers in Figs. 10 and 11.

Reference	Old λ	New λ	CNOF E_c	$Z \geq 10$ E_c	New E_c	Flux in particles/m ² sterad sec	
						CNOF	$Z \geq 10$
1	60°	62°	0.26a	0.35a		11.5 ± 1.0	7.9 ± 1.1
2	55°	55°	0.30	0.48a		10.4 ± 2	3.5 ± 1.0
3	55°	55°	0.30	0.55a		14.4 ± 1.4	4.2 ± 1.0
4	55°	55°	0.30	0.58a		12 ± 1	4.2 ± 0.7
5	55°	55°	0.30	0.35		15 ± 3	6.5 ± 1.0
6	55°	55°		0.53a			4.5 ± 0.5
7	55°	55°	0.30	0.48a		11.0 ± 1.6	3.5 ± 1.4
8	51°	48°	0.54	0.54	0.80	11.5 ± 3	4.0 ± 0.8
9	41.7°	44°	1.8	1.8	1.55	5.9 ± 0.7	2.4 ± 0.3
10	41°	43°	1.85	1.85	1.65	6.7 ± 1.2	3.0 ± 1.0
11	41°	43°		1.85	1.65		2.1 ± 0.3
12	41°	34°	1.75	1.75	3.1	2.8 ± 0.65	1.2 ± 0.4
13	30°	27°	3.85	3.85	4.3	3.3 ± 0.6	1.2 ± 0.4
14	30°	27°	3.85	3.85	4.3	3.9 ± 0.7	0.85 ± 0.1
15	10°	10°	6.1	6.1	6.1	1.1 ± 0.2	0.36 ± 0.06
16	10°	10°	6.1	6.1	6.1	0.68 ± 0.2	0.21 ± 0.05
17	3°	1°	6.4	6.4	6.5	1.23 ± 0.25	0.35 ± 0.08

* The "a" after a value means that the cutoff energy is imposed by the air above the detector rather than by the earth's magnetic field.

1. J. E. Naugle *et al.* (unpublished).

2, 8, 13 H. L. Bradt and B. Peters, *Phys. Rev.* **77**, 62 (1950).

3, 9 M. F. Kaplon *et al.*, *Phys. Rev.* **85**, 304 (1952).

4 A. D. Dainton *et al.*, *Phil. Mag.* **43**, 729 (1952).

5, 14 P. S. Freier *et al.*, *Phys. Rev.* **84**, 322 (1951).

6 G. W. Anderson *et al.*, *Phys. Rev.* **94**, 1317 (1954).

7, 10 M. F. Kaplon *et al.*, *Phys. Rev.* **96**, 1408 (1954).

11 P. S. Freier *et al.* (unpublished).

12 H. Fay, *Z. Naturforsch.* **10a**, 572 (1955).

13 J. J. Lord *et al.* (private communication).

16 R. E. Danielson *et al.* (present work).

17 D. Lal *et al.*, *Phys. Rev.* **86**, 570 (1952).

a power spectrum with an exponent of 2.0 or greater at $\lambda=10^\circ\text{N}$.

It should be noted in Figs. 10 and 11 that the flux value No. 12 measured over Europe is brought into much better agreement with other flux measurements when it is plotted at the "new" cutoff energy. As far as possible it would be desirable in the future to have a direct measurement of the cutoff energy when measuring a flux value. This is not possible at high energies but is possible at energies below about 1.5 Bev/nucleon.

ACKNOWLEDGMENTS

The authors wish to thank the Office of Naval Research for sponsoring Project Churchy and, in particular, Lieutenant-Commander M. D. Ross. We also want to thank Mrs. Dawn Copeland, Miss Pamela Curry, Miss Helene Colander, Miss Janet Witchell, and Mrs. LaDonna Wagner for the scanning of the emulsions.